A BRIEF REVIEW ON EIGHT FLAME SPREAD MODELS

C.W. Leung
Department of Building Services Engineering, The Hong Kong Polytechnic University, Hong Kong, China

ABSTRACT

Flame spread plays an important role in the fire growth in compartments. Mathematical models have been developed to study the flame spread problems in concurrent flow and opposed flow under different fire scenarios. In this paper, eight flame spread models in the literature were surveyed. The key equations were identified, the basic modelling logic and the use of material properties data determined in bench-scale tests including the cone calorimeter test and LIFT test were introduced.

1. BACKGROUND

Flame spread is the second step in fire growth following ignition. It is a major element in controlling the fire development and heat release rate. A key factor affecting the rate of flame spread is the heat transfer from the flame to the unburned material ahead of the flame for solid pyrolysis. This is strongly affected by the shape of the flame and the gas flow. Two modes of flame spread, i.e. concurrent flow flame spread and opposed flow flame spread have been classified [1]. Studies on flame spread problems have been carried out based on these two categories.

In concurrent flow flame spread, the flame propagates in the same direction as the oxidizing gas flow which can be natural wind or forced convective flow due to the buoyancy force induced by the fire itself. The flame is pushed ahead of the pyrolysis region and covers the unburned fuel surface while the solid is heated and pyrolyzed. This is similar to a rapid pilot ignition process which enhances a more rapid or even an accelerating rate of spread. A typical example is upward flame spread over a vertical surface.

In opposed flow flame spread, the flame spread over the fuel surface opposing to the flow of gaseous oxidizer, either naturally induced or forced. The flame is kept close to the surface downstream of the pyrolysis front, deterring the heat transferred ahead of the flame. The rates of spread are generally small and constant due to such difficulty in transferring the heat ahead of the flame. Examples are downward and horizontal flame spread in natural convection. A standard test ASTM E1321 LIFT test [2] was developed and well-used to study opposed flow spread problems.

A flame spread problem can be studied as a continuous ignition process where the flame front acts as the heat source to preheat and ignite the materials ahead. The ignition of the material can be divided into two mechanisms: solid phase heating and gasification, and gas phase chemical reactions of the pyrolyzed fuel vapour and oxidizer gas. The ignition time, t_{ig} is composed of the solid phase pyrolysis time, t_p and the gas phase induction time, t_{in}. In flame spread, since the flame itself is a pilot ignition front, the gas induction time is small especially in concurrent flow flame spread, such that $t_{ig} \sim t_p$ and the chemical kinetic effects are usually neglected in concurrent flame spread models for simplification. t_{ig} can be derived from the linear flow conduction equation for semi-infinite solids [3] such that

$$t_{ig} = \frac{\pi k \rho c \left(T_{ig} - T_o\right)^2}{4 \dot{q}_e''^2} \tag{1}$$

$\dot{q}_e''$ (in kWm^{-2}) is the total external heat flux.

2. FLAME SPREAD MODELS

Eight flame spread models [4-11] are reviewed. Those include

1) concurrent flow flame spread models developed by
   - Saito, Quintiere and Williams (1985) [4]
   - Hasemi and Yasni (1995) [5]
   - Grant and Drysdale (1995) [6]
2) opposed flow model developed by Quintiere in the LIFT test (1984) [7]
3) room-corner flame spread models developed by
   - Göransson and Wichström (1990) [8]
   - Karlsson (1992) [9]
   - Quintiere (1993) [10], and
4) flame spread models on LIFT using data from the cone calorimeter test [11] by
   - Qian (1990) [12]
   - Leung, Yuen and Chow (2003) [13].

The key equations are summarized and compared in Tables 1 to 4.

Table 1: Key equations in models on concurrent [4-6] and opposed flame spread [2]

- The rate of flame spread,

$$V_p(t) = \frac{x_f - x_p}{\tau} \qquad (2)$$

- Pyrolysis length,

$$x_p(t) = x_{po} + \int_0^t V_p(t_p)dt_p \qquad (3)$$

Model	Flame length	Burnout front	Concurrent flow flame spread rate
SQW [4], Scenario: Concurrent flame spread over a vertical surface	$x_f(t) = K\left(\dot{Q}_{ig} + \dot{Q}_m(t)\right)^n$ (4) • Linear n-power correlation: $n = 1$	-	The SQW equation: $V_p(t) = \frac{1}{\tau}\left\{ K\left[\dot{Q}_{ig} + x_{po}\dot{Q}'_m(t) + \int_0^t \dot{Q}'_m(t-t_p)V_p(t_p)dt_p\right]^n - \left[x_{po} + \int_0^t V_p(t_p)dt_p\right]\right\}$ (6)
Hasemi & Yasni [5], Scenario: Concurrent flame spread over a vertical surface	$x_f = K\left[\dot{Q}'_m(t) + \dot{Q}_{ig}(t)\right] + x_b$ (7) • Linear n-power correlation: $n = 1$	$x_b = \int_{t_b}^t V_p(t_p - t_b)dt_p + x_{po}$ (8)	$V_p(t) = \frac{1}{\tau}\left\{ K\left[\dot{Q}_{ig}(t)\left[1 - U(t-t_b)\right] + x_{po}\dot{Q}'_m(t) + \int_0^t \dot{Q}'_m(t-t_p)V_p(t_p)dt_p\right] + \left[\int_0^{t-t_b} V_p(t_p)dt_p + x_{p,o}\right]U(t-t_b) - \left[x_{po} + \int_0^t V_p(t_p)dt_p\right]\right\}$ (11)
Grant & Drysdate [6], Scenario: Concurrent flame spread over a vertical surface	• For $t < t_b$, Use Eq. (4) • For $t \geq t_b$, $x_f(t) = x_b + K\left[\dot{Q}_m(t)\right]^n$ (10) • Non-linear n-power correlation: $n = 2/3$	$x_b(t) = x_p(t - t_b)$ (9)	• For $t < t_b$, Use Eq. (6) • For $t \geq t_b$, $V_p(t) = \frac{1}{\tau}\left\{ K\left[\int_{t-t_b}^t \dot{Q}''_m(t-t_p)V_p(t_p)dt_p\right]^n - \int_{t-t_b}^t V_p(t_p)dt_p\right\}$ (12)
			Opposed flow flame spread rate
ASTM E1321 LIFT test [2]	-	-	$V_p = \frac{\Phi}{k\rho c\left(T_{ig} - T_s\right)^2}$ (15)

Table 2: Summary on input data and assumptions in models on ISO 9705 full-scale room-corner fire test [8-10]

	Göransson and Wichström [8], Simulation on pyrolysis area only; Materials mounted on ceiling and 3 walls	Karlsson [9], Model **A** - Concurrent flame spread; Materials mounted on ceiling and 3 walls	Karlsson [9], Model **B** - Concurrent and downward flame spread; Materials mounted on 3 walls	Quintiere [10], Concurrent, lateral and downward flame spread; Materials mounted on ceiling and 3 walls
Input data	• Cone calorimeter test (25 kWm^{-2}): t_{ig} , $\dot{Q}''_{cone}(t)$, $k\rho c$	• Cone calorimeter test (50 kWm^{-2}): $\dot{Q}''_{cone}(t)$ • Cone calorimeter/ LIFT test: T_{ig} , $k\rho c$	• Cone calorimeter test(50 kWm^{-2}) $\dot{Q}''_{\max}$ • LIFT test: Φ • Cone calorimeter/ LIFT test: T_{ig} , $k\rho c$	• Cone calorimeter test (50 kWm^{-2}): $\frac{\Delta H_c}{L}$ • LIFT test: Φ , $T_{s.\min}$ • Cone calorimeter/ LIFT test: T_{ig} , $k\rho c$
Assumed figures	• $\dot{Q}_{ig} = \begin{cases} 100kW, 0 < t \le 600s \\ 300kW, 600s < t \le 1200s \end{cases}$ • h_c = 0.05 kW(m^{2}K)$^{-1}$ • Wall area behind burner, $A_o = \begin{cases} 2m^2 , \dot{Q}_{ig} = 100kW \\ 5m^2 , \dot{Q}_{ig} = 300kW \end{cases}$ • Empirical constant in correlation of $A(t)$, $\alpha = \begin{cases} 0.05m^2s^{-1} , \dot{Q}_{ig} = 100kW \\ 0.5m^2s^{-1} , \dot{Q}_{ig} = 300kW \end{cases}$ • Proportionality factor in gas temperature correlation, γ = 50 K(W)$^{-0.4}$	$\dot{Q}_{ig} = \begin{cases} 100kW, 0 < t \le 600s \\ 300kW, 600s < t \le 1200s \end{cases}$ • Wall area behind burner, A_w = 0.71 m^2 • Flame length correlation: K = 0.01 m^{2}kW^{-1}, n = 1 • Pre-exponential coefficient in gas temperature correlation, C = 2.8	• $\dot{Q}_{ig} = 100kW$ • Flame temperature, T_f = 1100 K • Pyrolyzing material temperature, T_p = 750 K • Flame extension correlation: L_o = 0.4 m, K = 0.008 mkW^{-1} • Strip width in ceiling-wall intersection, W = 0.0753H = 0.18 m • Length of downward burning strip, L = length of walls • Burner heat flux, $\dot{q}''_{ig} = 45kWm^{-2}$ • Flame heat flux, $\dot{q}''_f = 35kWm^{-2}$ • Emission coefficient, ε = 1	• $\dot{Q}_{ig} = \begin{cases} 100kW, 0 < t \le 600s \\ 300kW, 600s < t \le 1200s \end{cases}$ • Flame length correlation: K = 0.01 m^{2}kW^{-1}, n = 1 • Flame length, $y_{po} = \begin{cases} 1.3m , \dot{Q}_{ig} = 100kW \\ 3.6m , \dot{Q}_{ig} = 300kW \end{cases}$ • x_{po} = 0.17 m • $\dot{q}''_f = \begin{cases} 60kWm^{-2}, pyrolysis\ area \\ 30kWm^{-2}, extended\ flame\ length \end{cases}$ • $\dot{q}''_{ig}$ = 60 kWm^{-2} • Pre-exponential coefficient in gas temperature correlation, C = 2.2 • Convective heat transfer coefficient, h_c = 0.01 kW(m^{2}K)$^{-1}$ • Ceiling jet region = 0.083H = 0.192 m • Ceiling area, wd = 8.64 m^2
Output	Heat release rate, $\dot{Q}_{tot}(t)$			

Table 3: Key equations in models on room-corner fire tests [8-10] – Heat release rate and flame spread velocity

- Total heat release rate,
  $\dot{Q}_{tot}(t) = \dot{Q}_{ig}(t) + \dot{Q}''_m A_p(t)$ (16) where $\dot{Q}_{ig}(t)$ is the heat given out by the burner, $\dot{Q}''_m$ is the heat release rate per unit area of pyrolysis material and $A_p(t)$ is the pyrolysis area.

Model	Heat release rate		Pyrolysis area, A_p (m^2)	Flame spread velocity (ms^{-1})
	Burner, $\dot{Q}_{ig}$ (kW)	Material, $\dot{Q}''_m$ (kWm^{-2})		
Göransson & Wichström [8], Scenario: Materials mounted on ceiling and 3 walls in ISO 9705	$\dot{Q}_{ig} = \begin{cases} 100kW, & 0 < t \le 600s \\ 300kW, & 600s < t \le 1200s \end{cases}$ if no flashover	Heat release rate data from cone calorimeter test (under 25 kWm^{-2}), $\dot{Q}''_{cone}(t)$	$A_p(t) = \begin{cases} A_o & ,\theta < \theta_s \\ A_o + \alpha\left(\frac{t}{t_{ig}}\right)^2 & ,\theta \ge \theta_s \end{cases}$ (17)	-
	Total heat release rate, $\dot{Q}_{tot}(t) = \dot{Q}_{ig} + \sum_{i=1}^{N} \Delta A_p{}^i \dot{Q}''_{cone}(t)^{N-i}$ (20)			
Karlsson [9], 2 Scenarios: Model **A** - Concurrent flame spread; Materials mounted on ceiling and 3 walls in ISO 9705 Model **B** - Concurrent and downward flame spread; Materials mounted on 3 walls in ISO 9705	• Model **A** $\dot{Q}_{ig} = \begin{cases} 100kW, & 0 < t \le 600s \\ 300kW, & 600s < t \le 1200s \end{cases}$ if no flashover • Model **B** $\dot{Q}_{ig}$ = 100 kW for all t (for simplification)	• Model **A** Heat release rate data from cone calorimeter test (under 50 kWm^{-2}), $\dot{Q}''_{cone}(t)$ • Model **B** Mathematical approximation, $\dot{Q}''_m = \dot{Q}''_{\max} e^{-\lambda(t-\tau)}$ (21) Decay coefficient, $\lambda(t) = avg\left[-\frac{1}{t}\ln\frac{\dot{Q}''_{cone}(t)}{\dot{Q}''_{\max}}\right]$ (22)	• Models **A** and **B** Upward flame spread region behind burner, A_w = constant = $23W_b 3H_w$ = 0.71 m^2 • Model **A** Initial ceiling pyrolysis area, $A_o = \dot{Q}_{ig} + \dot{Q}''_{\max} A_w e^{-\lambda(t-\tau)} - 150$ (34) Ceiling pyrolysis area, $A_p(t) = A_o + \int_0^t V(t)dt$	• Model **A** - Concurrent flame spread under ceiling, $V_A(t) = \frac{1}{\tau}\left\{\begin{array}{l} A_o + K\left[\begin{array}{l} A_o \dot{Q}''_{cone}(t) \\ + \int_0^t \dot{Q}''_{cone}(t-t_p) V_A(t_p) dt_p \end{array}\right] \\ -\left[A_o + \int_0^t V_A(t_p)dt_p\right] \end{array}\right\}$ (31) $\tau = \frac{\pi k\rho c (T_{ig} - T_s)^2}{4\dot{q}''^2_f}$ (32) • Linear n-power correlation: n = 1

Model	Heat release rate		Pyrolysis area, A_p (m^2)	Flame spread velocity (ms^{-1})
	Burner, $\dot{Q}_{ig}$ (kW)	Material, $\dot{Q}''_m$ (kWm^{-2})		
Karlsson [9], 2 Scenarios: Model **A** - Concurrent flame spread; Materials mounted on ceiling and 3 walls in ISO 9705 Model **B** - Concurrent and downward flame spread; Materials mounted on 3 walls in ISO 9705			• Model **B** Initial ceiling-wall intersection strip, $x_{po}W$ Ceiling-wall intersection strip, $W\int_0^{t_1} V_h(t_p)dt_p$ Downward burning strip, $L\int_0^{t_2} V_d(t_p)dt_p$	• Model **B** - Concurrent flame spread over horizontal ceiling-wall intersection, Flame length, $x_f = -L_o + K\dot{Q}_{tot}$ (35) $V_h(t) = \frac{1}{s_1 - s_2}\left[(B + As_1)e^{s_1 t} - (B + As2)e^{s_2 t}\right]$ (36) $A = \frac{1}{\tau}\left[-L_o + K\left(\dot{Q}_{ig} + A_w\dot{Q}''_{\max}e^{-\lambda\tau} + \dot{Q}''_{\max}Wx_{po}\right) - x_{po}\right]$ $B = \frac{\lambda}{\tau}\left(-L_o + K\dot{Q}_{ig} - x_{po}\right)$, $C = \frac{1}{\tau}\left(1 - K\dot{Q}''_{\max}W + \tau\lambda\right)$ $D = \frac{\lambda}{\tau}$, $s_1 = \frac{1}{2}\left(-C + \sqrt{C^2 - 4D}\right)$, $s_2 = \frac{1}{2}\left(-C - \sqrt{C^2 - 4D}\right)$ $\tau = \frac{\pi k\rho c(T_{ig} - T_o)^2}{4\dot{q}''^2_f}$ (37) • Model **B** - Downward flame spread, $V_d = \frac{\Phi}{k\rho c(T_{ig} - T_{fl,f})^2}$ (38)
	Total heat release rate, • Model **A** : $\dot{Q}_{tot,A}(t) = \begin{cases} \dot{Q}_{ig} & ,t < \tau_o \\ \dot{Q}_{ig} + A_w\dot{Q}''_{cone}(t-\tau_o) + A_o\dot{Q}''_{cone}(t_1) + \int_0^t \dot{Q}''_{cone}(t_1 - t_p)V_A(t_p)dt_p & ,t > \tau_o \end{cases}$ (33) • Model **B** : $\dot{Q}_{tot,B}(t) = \begin{cases} \dot{Q}_{ig} & ,t < \tau_o \\ \dot{Q}_{ig} + A_w\dot{Q}''_{\max}e^{-\lambda(t-\tau_o)} + x_{po}W\dot{Q}''_{\max}e^{-\lambda t_2} + W\int_0^{t_1}\dot{Q}''_{\max}e^{-\lambda(t_1-t_p)}V_h(t_p)dt_p + L\int_0^{t_2}\dot{Q}''_{\max}e^{-\lambda(t_2-t_p)}V_d(t_p)dt_p & ,t > \tau_o \end{cases}$ (39) Ignition time of A_w, $\tau_o = \frac{\pi k\rho c(T_{ig} - T_o)^2}{4\dot{q}''^2_{ig}}$ (23) $t_1 = t - (\tau_o + \tau)$, τ = ignition time of A_o $t_2 = t - t_d$, t_d = time at onset of downward flame spread			

Model	Heat release rate		Pyrolysis area, A_p (m^2)	Flame spread velocity (ms^{-1})
	Burner, $\dot{Q}_{ig}$ (kW)	Material, $\dot{Q}''_m$ (kWm^{-2})		
Quintiere [10], Scenario: Concurrent, lateral and downward flame spread; Materials mounted on ceiling and 3 walls in ISO 9705	$\dot{Q}_{ig} = \begin{cases} 100kW, & 0 < t \le 600s \\ 300kW, & 600s < t \le 1200s \end{cases}$ if no flashover	$\dot{Q}''_m = \frac{\Delta H}{L}(\dot{q}''_f - \sigma T_{ig}{}^4 + \sigma T_g{}^4)$ (40)	$A_p = A_{p1} - A_{p2} + A_{pj1} + A_{pc1}$ (52) • Wall pyrolysis area, $A_{p1} = 2\left[Hx_{po} + (x_p - x_{po})y_{po} + \frac{1}{2}(H - y_{po})(x_p - x_{po})\right]$ (53) • Burnout area, $A_{p2} = 2\left[y_p x_{po} + (x_b - x_{po})y_{po} + \frac{1}{2}(y_b - y_{po})(x_b - x_{po})\right]$ (54) • Wall pyrolysis area associated with the ceiling jet, $A_{pj1} = 2\left[0.08H(y_b - H) + \frac{1}{2}z_p(y_b - H) - \frac{1}{2}\frac{(0.08H + z_p)^2(x_p - x_{po})}{(H - y_{po})}\right]$ (55) • Ceiling pyrolysis area, $A_{pc1} = \min\left[\frac{\pi}{4}(y_p - H)^2, wd\right]$ (56)	• Upward flame spread rate, $\frac{dy_p}{dt} = \frac{y_f - y_p}{\tau}$ (45) $\tau = \frac{\pi k\rho c(T_{ig} - T_s)^2}{4\dot{q}''^2_f}$ (32) Extended flame heat flux beyond the burning region, $\dot{q}''_f$ = 30 kWm^{-2} Upward flame length (in wind-aided direction), $y_f = \begin{cases} y_b + K\left[\dot{Q}'_{ig} + \dot{Q}''_m(y_p - y_b)\right]^n & , y_b \le K\dot{Q}'^n_{ig} \\ y_b + K\left[\dot{Q}''_m(y_p - y_b)\right]^n & y_b \ge K\dot{Q}'^n_{ig} \end{cases}$ (46) • Linear n-power correlation: $n = 1$ • Upward burn-out rate, $\frac{dy_b}{dt} \approx \frac{y_p(t) - y_b(t)}{t_b}$ (47) Burnout time, $t_b = \frac{Q''_m}{\dot{Q}''_m}$ (44) $t_{b,o} = \frac{Q''_m}{\dot{Q}''_m(\tau_o)}$

Model	Heat release rate		Pyrolysis area, A_p (m^2)	Flame spread velocity (ms^{-1})
	Burner, $\dot{Q}_{ig}$ (kW)	Material, $\dot{Q}''_m$ (kWm^{-2})		
Quintiere [10], Scenario: Concurrent, lateral and downward flame spread; Materials mounted on ceiling and 3 walls in ISO 9705			Initial conditions, • For $0 \le t < \tau_o$, $y_p = x_p = 0$ • When $t = \tau_o$, $y_p = y_{po} = 1.3$ m, $x_p = x_{po} = 0.17$ m • For $0 \le t < (\tau_o + t_{b,o})$, $y_b = x_b = 0$ • When $t = (\tau_o + t_{b,o})$, $x_b = x_{po}$, $y_b = y_{po}$ • For $0 \le t \le t_H$, $z_p = 0$ • For $0 \le t \le t'_H$, $z_b = 0$	• Lateral flame spread rate, $\frac{dx_p}{dt} = \left[\frac{\Phi}{k\rho c(T_{ig} - T_s)^2}\right]$ for $T_s \ge T_{s,\min}$ (48) • Lateral burn-out rate, $\frac{dx_b}{dt} \approx \frac{x_p(t) - x_b(t)}{t_b}$ (49) • Downward flame front, $z_p = y_p(t) - y_p(t_H)$ at $t > t_H$ when $y_p = H$ (50) • Downward burn-out front, $z_b = y_b(t) - y_b(t'_H)$ at t'_H is the time when $y_b = H$ (51)
	Total heat release rate, $\dot{Q}_{tot}(t) = \begin{cases} \dot{Q}_{ig} & , t < \tau_o \\ \dot{Q}_{ig} + \dot{Q}''_m A_p(t) & , t > \tau_o \end{cases}$ (16)		τ_o is the time when $T_{s,o} = T_{ig}$	

Table 4: Key equations in models on room-corner fire tests [8-10] – Upper layer gas temperature and surface temperature

Model	Upper layer gas temperature	Surface temperature
Göransson & Wichström [8]	Gas temperature, $\theta_g(t) = \gamma Q_{tot}^{\frac{2}{5}}$ (19)	$\theta_s(t) = \sum_{i=1}^{N} \theta_g{}^{i} \eta^{N-i}$ (18) Response function, $\eta = \frac{\theta_s}{\theta_g} = 1 - \exp(t - t_g) erfc\left[\left(\frac{t}{t_g}\right)^{0.5}\right]$ $t_g = \frac{k\rho c}{h_c{}^2}$
Karlsson [9]	$\frac{T_g - T_o}{T_o} = 2.8\left[\frac{\dot{Q}_{tot}}{\rho_o c_p \sqrt{g} T_o A_o \sqrt{H_o}}\right]^{\frac{2}{3}}\left[\frac{h_k A_w}{\rho_o c_p \sqrt{g} T_o A_o \sqrt{H_o}}\right]^{-\frac{1}{3}}$ (24) Heat transfer coefficient, $h_k = \sqrt{\frac{k\rho c}{t}}$ • Models **A** and **B** - Instantaneous gas layer heat flux (*g*) before downward flame spread, $\dot{q}'' = \varepsilon F \sigma (T_g^4 - T_o^4)$ (25) • Model **B** - Instantaneous gas layer heat flux (*g*) + Radiation from wall flame (*f*) and pyrolyzing materials behind the flame (*p*) when downward flame spread starts, $\dot{q}'' = \varepsilon_g F_g \sigma (T_g^4 - T_o^4) + \varepsilon_f F_f \sigma (T_f^4 - T_o^4) + \varepsilon_p F_p \sigma (T_p^4 - T_o^4)$ (26)	• Models **A** and **B** - Materials inside the gas layer Boundary condition, $k\frac{\delta T}{\delta y}\Big\|_{y=0} = h(T_g - T_o)$ (29) $T_s(n) = T_o + \sum_{i=1}^{n}\left[T_g(i) - T_g(i-1)\right] \exp\left(\frac{h_N^2 (n-i) dt}{k\rho c}\right) erfc\left[h_N \sqrt{\frac{(n-i)dt}{k\rho c}}\right]$ (27) • Model **B** - Materials beneath the gas layer Boundary condition, $k\frac{\delta T}{\delta y}\Big\|_{y=0} = \dot{q}'' - h_N (T - T_o)$ (30) $T_s(n) = T_o + \sum_{i=1}^{n} \frac{\dot{q}''(i) - \dot{q}''(i-1)}{h_N} \exp\left(\frac{h_N^2 (n-i) dt}{k\rho c}\right) erfc\left[h_N \sqrt{\frac{(n-i)dt}{k\rho c}}\right]$ (28)
Quintiere [10]	$\frac{T_g - T_o}{T_o} = 2.2\left[\frac{\dot{Q}_{tot}}{\rho_o c_p \sqrt{g} T_o A_o \sqrt{H_o}}\right]^{\frac{2}{3}}\left[\frac{\sqrt{k\rho c / t} A_s}{\rho_o c_p \sqrt{g} T_o A_o \sqrt{H_o}}\right]^{-\frac{1}{3}}$ (42)	• For $t < \tau_o$, $T_{s,o} = T_o + \frac{1}{\sqrt{\pi k\rho c}} \int_0^t \frac{\dot{q}_{ig}'' + \sigma(T_g{}^4 - T_s^4)}{\sqrt{t - t_p}} dt_p$ (41) • For $t \geq \tau_o$, $T_s = T_o + \frac{1}{\sqrt{\pi k\rho c}} \int_0^t \frac{\sigma(T_g{}^4 - T_s{}^4) + h_c(T_g - T_s)}{\sqrt{t - t_p}} dt_p$ (43)

3. CONCURRENT FLOW FLAME SPREAD MODELS

Upward flame spread over a vertical surface have been generally used to represent a concurrent flame spread problem and taken as the modelling scenario. The modelling results are applied to other cases in concurrent flow, including flame spread along a ceiling-wall intersection and beneath a horizontal ceiling.

3.1 Concurrent Flame Spread Model Without Burnout Effect

Saito, Quintiere and Williams (SQW) [4] studied the two-dimensional concurrent upward flame spread over a vertical thermally thick surface under a turbulent flow. Materials were assumed to be thick enough that burnout was not considered. It was considered as a quasi-steady state burning starting from the base of the vertical surface. Heat loss at the unexposed side and the chemical kinetics were ignored. The flame spread model is shown in Fig. 1.

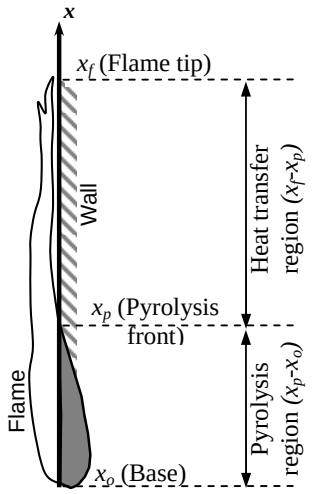

Fig. 1: Upward flame spread model by SQW [4]

The heat flux from the flame, $\dot{q}''_f$ to the solid surface was assumed to be constant over $x_p < x \le x_f$ which is the only heat transfer region to raise the fuel surface temperature to the ignition temperature, T_{ig} for further flame spread. No heat is transferred to the fuel beyond x_f. The region $(x_f - x_p)$ was assumed to be approximately constant as the flame spreads. The rate of flame spread was defined as

$$V_p(t) = \frac{x_f - x_p}{\tau} \tag{2}$$

τ (in s) is the characteristic ignition time, i.e. the time necessary for the region $(x_f - x_p)$ to be ignited by the flame heat flux above it. It is determined by Eq. (1).

To obtain $V_p(t)$ (in ms^{-1}), expressions for x_f (in m) and x_p (in m) should be obtained. By definition,

$$x_p(t) = x_{po} + \int_0^t V_p(t_p)dt_p \tag{3}$$

where x_{po} is x_p at $t = 0$ and t_p is a dummy variable.

The flame height was found [e.g. 14] to be proportional to the heat release rate in a power-n law,

$$x_f(t) = K\left[\dot{Q}_{tot}(t)\right]^n \tag{4}$$

K (in mkW^{-1}) is a constant related to the fire location such as fire at the centre of a room, in a corner or at an open wall, and the environmental conditions including air entrainment to the fire plume. $\dot{Q}_{tot}(t)$ is the total heat flux from the pilot flame, $\dot{Q}_{ig}$ and the heat release rate from the burning part of the fuel after ignition, $\dot{Q}_m(t)$, i.e. $\dot{Q}_{tot}(t) = \dot{Q}_{ig} + \dot{Q}_m(t)$ and

$$\dot{Q}_m(t) = x_{po}\dot{Q}'_m(t) + \int_0^t \dot{Q}'_m(t - t_p)V_p(t_p)dt_p \tag{5}$$

$\dot{Q}'_m(t)$ (in kWm^{-1}) is the heat release rate of the material per unit width of the flame front.

Putting Eqs. (3) to (5) into Eq. (2), $V_p(t)$ was derived,

$$V_p(t) = \frac{1}{\tau}\left\{K\left[\dot{Q}_{ig} + x_{po}\dot{Q}'_m(t) + \int_0^t \dot{Q}'_m(t - t_p)V_p(t_p)dt_p\right]^n - \left[x_{po} + \int_0^t V_p(t_p)dt_p\right]\right\} \tag{6}$$

This is referred to as the SQW equation. It has been commonly used in analyzing concurrent flow flame spread problems. The power n was found to be 2/3 experimentally [e.g. 14-16] but it was taken as unity by SQW for simplified calculations and to provide roughly correct theoretical predictions [4].

3.2 Concurrent Flame Spread Model With Burnout Effect

In the SQW model, burnout was neglected. However, the burnout effect can be very significant especially for thin materials or plastic materials

with a short burning time. The SQW equation was revised [5,6] to include the burnout front, x_b and the local burnout time, t_b. The flame length (Eq. 4) was redefined by Hasemi and Yasni [5] as:

$$x_f = K[\dot{Q}_{ig}(t) + \dot{Q}_m(t)] + x_b \tag{7}$$

and

$$x_b = \int_{t_b}^{t} V_p(t_p - t_b)dt_p + x_{po} \tag{8}$$

Similarly, Grant and Drysdale redefined x_b as

$$x_b(t) = x_p(t - t_b) \tag{9}$$

For $t \geq t_b$, the flame height correlation $x_f(t) - x_b(t)$ becomes:

$$x_f(t) - x_p(t - t_b) = K\left[\dot{Q}_m(t)\right]^n \tag{10}$$

When the burnout front is larger than the flame length of the burner, the influence of $\dot{Q}_{ig}(t)$ to the fuel should be neglected. A rectangular function of time, $u(t) = 1 - U(t - t_b)$ was added in Hasemi's model to include this influence such that the SQW equation was revised as

$$V_p(t) = \frac{1}{\tau}\left\{\begin{array}{l} K\left[\dot{Q}_{ig}(t)\left[1 - U(t - t_b)\right] + x_{po}\dot{Q}'_m(t) + \int_0^t \dot{Q}'_m(t - t_p)V_p(t_p)dt_p\right] \\ + \left[\int_0^{t-t_b} V_p(t_p)dt_p + x_{p,o}\right]U(t - t_b) - \left[x_{po} + \int_0^t V_p(t_p)dt_p\right] \end{array}\right\} \tag{11}$$

In Grant's model, the SQW equation was used for $t < t_b$ and a revised equation including the burnout effect was used for $t \geq t_b$,

$$V_p(t) = \frac{1}{\tau}\left\{K\left[\int_{t-t_b}^{t} \dot{Q}'_m(t - t_p)V_p(t_p)dt_p\right]^n - \int_{t-t_b}^{t} V_p(t_p)dt_p\right\} \tag{12}$$

Numerical solutions were given for Eq.(12). This permits the direct use of the raw empirical heat release rate data and to retain the empirical 2/3-power flame length correlation. However, only a simplified lineralized flame length relationship was used in Hasemi's model (Eq. 11) for analytical solutions.

4. OPPOSED FLOW FLAME SPREAD MODEL

From Eqs. (1) and (2), Quintiere derived the solution of V_p as

$$V_p = (x_f - x_p)\left[\frac{\pi k\rho c(T_{ig} - T_s)^2}{4\dot{q}''^2_f}\right]^{-1} \tag{13}$$

$\dot{q}''_f$ is the flame heat flux and the temperature rise due to external heating.

de Ris [17] also derived the solution for opposed flow V_p under steady conditions including the solid and gas phases in two-dimensions,

$$V_p = V_g \frac{(k\rho c)_g}{k\rho c}\left(\frac{T_f - T_{ig}}{T_{ig} - T_s}\right)^2 \tag{14}$$

V_g (in ms^{-1}) is the opposed flow velocity, T_f is the flame temperature and the subscript g denotes gas phase properties.

From Eqs. (13) and (14), Quintiere derived a new material flame spread property, Φ such that

$$V_p = \frac{\Phi}{k\rho c(T_{ig} - T_s)^2} \tag{15}$$

Φ (in kW^2m^{-3}) was found to be a constant for a particular material under fixed V_g and ambient oxygen concentration. To determine Φ, the LIFT test [2] was developed by Quintiere [7]. Materials are mounted vertically opposite to a radiation panel giving an external radiant heat flux, $\dot{q}''_e$ as shown in Fig. 2. $\dot{q}''_e$ is set at 5 kWm^{-2} above the minimum heat flux for ignition, $\dot{q}''_{o,ig}$ (in kWm^{-2}) obtained in the ignition protocol of the test for the particular materials. The material is ignited at the hot end close to the radiation panel and the flame is allowed to spread laterally along the material. The flame spread distances with time are measured to determine the flame spread rate, $V_p(t)$. Φ can be derived from $V_p(t)^{-0.5}$, $\dot{q}''_e$ and $\dot{q}''_{o,ig}$. The readers are referred to the LIFT standard for the detail derivation. Eq. (15) has been commonly used to model opposed flow flame spread problems.

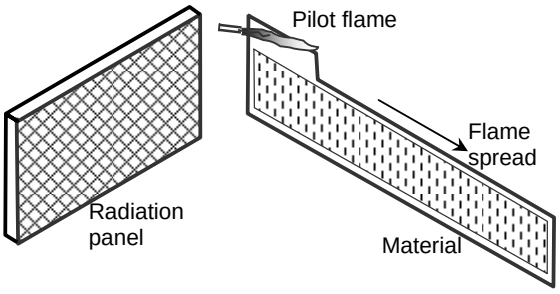

Fig. 2: Configuration of the LIFT test [2]

5. MODELS ON ROOM-CORNER FIRE SCENARIO

5.1 ISO 9705 Full-Scale Room-Corner Fire Test

ISO 9705 [18] is a test method that simulates a fire starting at a corner of a small well-ventilated room. In the standard test, materials are mounted on the ceiling and walls of a room 3.6 m long, 2.4 m wide and 2.4 m high. A door 0.8 m wide and 2.0 m high is opened on one of the walls, 2.4 m by 2.4 m as shown in Fig. 3. A gas hood is mounted on top of the door to collect all the combustibles during the test and connected to the duct section for determination of the heat release rate by the oxygen consumption method. A square gas burner of width 0.17 m and height 0.145 m is located at the rear wall corner to start the fire with heat output schedule, $\dot{Q}_{ig}(t)$ at 100 kW for 600 s and 300 kW for further 600 s if there is no flashover in the first 600 s. ISO 9705 have been recommended [e.g. 19] as an ideal full-scale test on assessing flame spread properties of materials.

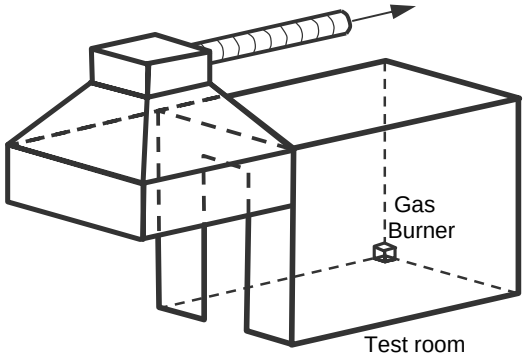

Fig. 3: Configuration of ISO 9705 [18]

Models were developed by Göransson and Wichström [8], Karlsson [9] and Quintiere [10] to simulate the flame spread inside the room. Göransson and Wichström [8] developed a simple model using data from the cone calorimeter test and empirical correlations on the burning area. The heat release rate, surface temperature and gas temperature inside the room were simulated. Karlsson and Quintiere's models used concurrent flow theories by SQW and opposed flow theories in LIFT for detail determination of the flame spread rates. The ignition, hot gas layer temperature, surface temperature of materials, burning area, heat release rate and time to flashover were simulated using input data from bench-scale tests including the LIFT test and the cone calorimeter test. In both of the models, materials were assumed as thermally thick, homogenous and of constant thermal properties with temperature. Chemical kinetics was excluded.

In those models, a general approach was used to estimate $\dot{Q}_{tot}(t)$ in the room. $\dot{Q}_{tot}(t)$ include the burner heat output, $\dot{Q}_{ig}(t)$ and the heat given out by the material during flame spread, $\dot{Q}_{m}(t)$. $\dot{Q}_{m}(t)$ was obtained by determining the burning area, $A_p(t)$ and the heat release rate per unit area of the material, $\dot{Q}''_m$ such that

$$\dot{Q}_m(t) = A_p(t) \cdot \dot{Q}''_m$$

and

$$\dot{Q}_{tot}(t) = A_p(t) \cdot \dot{Q}''_m + \dot{Q}_{ig}(t) \qquad (16)$$

Different approximations on $A_p(t)$ and $\dot{Q}''_m$ were made in the models [8-10]. The key assumptions and equations used in the models are summarized in Table 2 to 4.

5.2 Göransson and Wichström's Flame Spread Model on Room-Corner Fire Scenario

The flame spread rate was assumed to be dependent on the igniton time, t_{ig} of materials in the cone calorimeter test under 25 kWm^{-2} only. The area behind the burner flame, A_o was assumed to be first ignited. Simple empirical correlations were made on A_o and $A_p(t)$:

$$A_p(t) = \begin{cases} A_o & ,\theta < \theta_s \\ A_o + \alpha\left(\dfrac{t}{t_{ig}}\right)^2 & ,\theta \geq \theta_s \end{cases} \qquad (17)$$

$A_p(t)$ was assumed to grow as a t^2 function once an effective surface temperature, θ_s is reached. θ_s is dependent on the temperature of the combustion gases, θ_g passing by, the thermal response of the surface, and thus the thermal inertia, $k\rho c$ for semi-

infinite materials. α is an empirical constant. Equations on θ_s (Eq. 18) and θ_g (Eq. 19) are shown in Table 4.

The total heat release rate, $\dot{Q}_{tot}(t)$ was determined by Duhamel integral by

$$\dot{Q}_{tot}(t) = \dot{Q}_{ig} + \sum_{i=1}^{N} \Delta A_p{}^{i} \dot{Q}''_{cone}(t)^{N-i} \quad (20)$$

The heat release rate histories of materials in ISO 9705 were assumed to be the same as in the cone calorimeter under 25 kWm^{-2}, $\dot{Q}''_{cone}(t)$. Thus, the data from the cone calorimeter was directly used in Eq. (20) to replace $\dot{Q}''_m$ in Eq. (16).

5.3 Karlsson's Flame Spread Model on Room-Corner Fire Scenario

Two models were developed based on two scenarios A and B. Different flame spread patterns and assumptions on $\dot{Q}''_m$ were made in Models A and B. $A_p(t)$ was estimated based on the flame spread rate and thus the pyrolysis fronts.

- Model A

In scenario A, materials were attached on the ceiling and three walls following the ISO 9705 standard test method. It was assumed that the flame will spread upward starting from the ignition source at the rear corner of the room, followed by concurrent flow flame spread beneath the ceiling and leads to flashover. As a result, the simulation was focused on concurrent flame spread. Only the heat given out by the burner, burning of the vertical wall area behind the burner, ceiling, ceiling-wall intersection and the flame spread over those regions were simulated. Both downward and lateral flame spread were not considered. In Model A, numerical solutions were provided. The heat release rate curve from the cone calorimeter test, $\dot{Q}''_{cone}(t)$ can be used to replace $\dot{Q}''_m$ in Eq. (16) and no mathematical approximation was required. The standard burner schedules were followed in Model A.

Input parameters include $k\rho c$ and T_{ig} of the materials and the heat release rate obtained at 50 kWm^{-2} in the cone calorimeter test, $\dot{Q}''_{cone}(t)$.

- Model B

In scenario B, materials were mounted on the three walls of the room only. Flame was expected to spread upward from the burner and horizontally along the ceiling-wall intersection in concurrent flow and finally downward. Heat was given out by the burner, burning of the ceiling-wall intersection corresponding to the vertical height of the ceiling jet, wall materials inside and beneath the hot gas layer during downward flame spread. The heat released causing flashover in the room was assumed to be dominated by the heat given out during the downward flame spread. Both concurrent and downward flame spread were simulated. Analytical solutions were given in Model B such that approximations and simplifications were required. Only constant burner heat output, i.e. 100 kW was input in the model.

Input parameters include $k\rho c$, T_{ig}, the opposed flow flame heating parameter, Φ, heat release rate decay coefficient, λ and the peak heat release rate, $\dot{Q}''_{\max}$ obtained in the cone calorimeter.

The heat release rate from the burning material was approximated by

$$\dot{Q}''_m = \dot{Q}''_{\max} e^{-\lambda t} \quad (21)$$

λ is the decay coefficient determined from the peak heat release rate, $\dot{Q}''_{\max}$ and heat release rate data, $\dot{Q}''_{cone}(t)$ in the cone calorimeter under 50 kWm^{-2}. Only the first decaying part of the heat release rate curve from the cone calorimeter was used, especially for charring materials such as wood which usually have two peaks in the heat release rate.

$$\lambda(t) = avg\left[-\frac{1}{t} \ln \frac{\dot{Q}''_{cone}(t)}{\dot{Q}''_{\max}} \right] \quad (22)$$

In both scenarios, the heat flux from the flame and the pyrolyzing material were assumed to be constant. The wall area behind the burner, A_w (in m^2) was assumed to be ignited simultaneously due to the heat flux from the gas burner, $\dot{q}''_{ig}$ at τ_o (in s). τ_o (Eq. 23) was derived from Eq.(1) with $\dot{q}''_e = \dot{q}''_{ig}$. $\dot{q}''_{ig}$ was taken as 45 kWm^{-2}. A_w was taken as the width of the burner by the height between the burner surface to the ceiling, i.e. 0.71 m^2 in ISO 9705.

The wall and ceiling surfaces were divided into horizontal strips and the upper layer gas temperature, T_g, heat flux on the materials, $\dot{q}''$, surface temperature of materials, T_s, flame spread velocity, $V_p(t)$ and total heat release rate $\dot{Q}_{tot}(t)$ were calculated with respect to the location of the materials and time. Karlsson derived an expression on the upper layer gas temperature, T_g based on a regression equation developed by McCaffrey et al.

[20] with some modifications based on 41 experiments for scenarios A and B both in full scale and 1/3 scale tests [21] and adopted a correlation coefficient of 2.8.

$$\frac{T_g - T_o}{T_o} = 2.8\left[\frac{\dot{Q}_{tot}}{\rho_o c_p \sqrt{g} T_o A_o \sqrt{H_o}}\right]^{\frac{2}{3}}\left[\frac{h_k A_w}{\rho_o c_p \sqrt{g} T_o A_o \sqrt{H_o}}\right]^{-\frac{1}{3}} \quad (24)$$

T_g was used to determine the instantaneous gas layer *(g)* heat flux incident on the wall (Eq. 25). The gas layer was assumed to stabilize at the door height, i.e. 2 m. The heat flux from the gas layer on the centre of each wall strip was stimulated. In Model A, since it was assumed that the flame spread over the ceiling is dominant for leading flashover in the room and downward flame spread over the walls were not simulated, the heat flux and surface temperature of wall surfaces below the gas layer was not calculated. In Model B, the simulation of the downward spread is important. The radiation from the wall flame *(f)* and the pyrolyzing materials *(p)* behind the flame should be added once downward spread starts, such that the total heat flux on the wall strips includes 3 components (Eq. 26). Based on the total heat flux on each strip, the surface temperatures of wall materials inside (Eq. 27) and beneath the hot gas layer (Eq. 28) were determined by solving the one-dimensional heat conduction with different boundary conditions (Eqs. 29,30) by Laplace transform [3]. The wall and ceiling materials immersed in the hot gas layer were assumed to be heated by the hot gas alone and there is only one temperature per time step. By ignoring the re-radiation, the surface temperature of materials beneath the gas layer, T_s at time step n is a function of time and height from the floor and was calculated using the superposition principle based on the heat flux at each strip. The equations on T_g and T_s are showed in Table 4.

Thomas and Karlsson [22] rewrote the SQW equation in area (in m^2) based on Parker's expression [23] developed for the one-dimensional flame spread problem in the ASTM E84 tunnel test configuration [24]. This was used to model the concurrent flame spread velocity under the ceiling, $V_A(t)$ (in m^2s^{-1}) in Model A and was solved numerically. The heat release rate curve from the cone calorimeter at time t after ignition, $\dot{Q}''_{cone}(t)$ was directly used. A quasi-steady state was assumed and the equation on $V_A(t)$ (Eq. 31) was solved by iteration. K was taken as 0.01 m^2kW^{-1} in the flame length correlation [25]. To include the preheat from the hot gas layer, T_s was used, instead of T_o in Eq. (1) with $\dot{q}''_e = \dot{q}''_f$ to determine the ignition time, τ (Eq. 32). The heat flux from the flame, $\dot{q}''_f$ was taken as 35 kWm^{-2}.

The total heat release rate in Model A includes the heat given out by the ignition source, burning of A_w and the ceiling, i.e.

$$\dot{Q}_{tot,A}(t) = \dot{Q}_{ig} + A_w \dot{Q}''_{cone}(t - \tau_o) + A_o \dot{Q}''_{cone}(t_1) + \int_0^t \dot{Q}''_{cone}(t_1 - t_p) V_A(t_p) dt_p \quad (33)$$

where $t_1 = t - (\tau_o + \tau)$; τ_o is the ignition time of A_w and τ is the ignition time of the initial ceiling pyrolysis area, A_o (Eq. 34) caused by the flame extension under the ceiling. The heat loss from the fire plume at corner was taken as 150 kW.

In Model B, the concurrent flow flame spread in the ceiling-wall intersection was determined analytically using the flame extension correlation (Eq. 35). The ceiling-wall intersection, W was taken as 7.5% of the room height. Mathematical approximation, $\dot{Q}''_{\max}(t)e^{-\lambda t}$ was used and the preheating by the hot gas layer was neglected for simplification. The flame length and flame extension beneath the ceiling were determined and the flame spread velocity in the horizontal ceiling-wall intersection, V_h (Eq. 36) was determined by the SQW equation (in area) and solved analytically. The ignition time, τ was determined by Eq. (37). Since preheating by the gas layer was not considered in Model B, T_o was used. The assumptions on $\dot{q}''_f$ were the same as in Model A in Eq. (32).

The downward spread was assumed to start when the flame spread along the ceiling-wall intersection reaches the opposite corner. The downward flame spread rate, V_d (Eq. 38) was determined based on the LIFT Eq. (15) and using the material surface temperature just ahead of the flame front, $T_{fl,f}$ to replace T_s. The total heat release rate includes the heat given out by the ignition source, $\dot{Q}_{ig}$ upward flame spread over A_w, horizontal spread along the ceiling-wall intersection and finally the downward flame spread over the walls, i.e.

$$\dot{Q}_{tot,B}(t) = \dot{Q}_{ig} + A_w \dot{Q}''_{\max} e^{-\lambda(t-\tau_o)} + x_{po} W \dot{Q}''_{\max} e^{-\lambda t_2} + W\int_0^{t_1} \dot{Q}''_{\max} e^{-\lambda(t_1 - t_p)} V_h(t_p) dt_p + L\int_0^{t_2} \dot{Q}''_{\max} e^{-\lambda(t_2 - t_p)} V_d(t_p) dt_p \quad (39)$$

where $t_2 = t - t_d$; t_d is the time at the onset of downward flame propagation. L (in m) is the length of the downward burning strips, taken as the length of the three walls of the rooms. Based on $\dot{Q}_{tot}(t)$, the time to flashover can be estimated.

5.4 Quintiere's Model on Room-Corner Fire Scenario

Burnout was not considered in Karlsson's model. In Quintiere's model, this was considered by estimating the burnout time and thus locating the burnout front of the materials. The concurrent flow flame spread upward along the vertical walls, ceiling, wall-ceiling jet region and the opposed flow laterally and downward flame spread were simulated. The flame spread was assumed to be symmetric in the corner over the two walls but no pre-defined spreading pattern was fixed as in Karlsson's model. The pyrolysis area, $A_p(t)$ was simulated depending on the locations of the pyrolysis and burnout fronts. Input data required include Φ and the minimum surface temperature for flame spread, $T_{s,min}$ derived from the LIFT test; T_{ig}, kpc determined from the LIFT test or in the cone calorimeter; and the effective material property, $\Delta H_c/L$ derived from the cone calorimeter data under 50 kWm^{-2}.

It was assumed that the burner heat flux, $\dot{q}''_{ig}$ incident on the wall area behind the burner defined by the width of the burner,0.17 m and the flame height is uniform, taken as 60 kWm^{-2} [26]. Flame lengths due to the burner output were taken [27] as 1.3 m at 100 kW and 3.6 m at 300 kW.

To determine $\dot{Q}''_m$ in Eq. (16), the materials were tested in the cone calorimeter under different values of external radiant heat flux. The peak heat release rate was found to be well-correlated with the external heat flux, such that the peak heat release rate under all flux conditions can be determined by:

$$\dot{Q}''_m = \frac{\Delta H}{L}(\dot{q}''_f - \sigma T_{ig}^{\ 4} + \sigma T_g^{\ 4}) \qquad (40)$$

$\dot{Q}''_m$ was assumed as a constant, independent of time and uniform over the pyrolysis area. It was only dependent on the heat flux from the flame, $\dot{q}''_f$ (in kWm^{-2}), room thermal feedback, $\sigma T_g^{\ 4}$ (in kWm^{-2}) and re-radiation loss, $\sigma T_{ig}^{\ 4}$ (in kWm^{-2}) occurring at the ignition temperature of the materials. $\dot{q}''_f$ was assumed to be 60 kWm^{-2} over the entire pyrolysis region. Melting of materials was not considered and uniform burning over the materials was assumed.

The material behind the burner was assumed to be ignited when the surface temperature, $T_{s,o}$ (Eq. 41) reaches the ignition temperature, T_{ig}. $T_{s,o}$ was calculated based on the radiative heat flux from the burner and the upper layer gas.

To determine the room thermal feedback, $q(t_p)$, the upper layer gas temperature, T_g (Eq. 42) was estimated by the regression equation developed by McCaffrey et al. [20,27]. This is similar to the Eq. (24) used by Karlsson but a different correlation coefficient of 2.2 was used. Blackbody radiation and unit configuration factor was used to maximize the room feedback effect. T_g and $T_{s,o}$ were determined until the wall is ignited by the burner. When $T_{s,o}$ reaches T_{ig}, the ignition time due to the burner flame, τ_o can be obtained. The surface temperature of the materials, T_s (Eq. 43) was then determined based on the radiative and convective heat flux from the gas layer.

The pyrolysis area, $A_p(t)$ is a function of the positions of the upward pyrolysis front and burnout front, y_p and y_b, lateral pyrolysis and burnout fronts, x_p and x_b, and the downward pyrolysis front, z_p. The burnout time, t_b (Eq. 44) was determined by dividing the constant total available energy per unit area, Q''_m determined from the cone calorimeter, by the heat release rate per unit area, $\dot{Q}''_m$. Downward flame spread was assumed to start at t_H when the upward pyrolysis front, y_p reaches the room height, H. The downward burnout was assumed to start at t'_H when the upward pyrolysis burnout front, y_b reaches H. The initial conditions of A_p are summarized in Table 3.

The concurrent pyrolysis rate (Eq. 45) was determined using the SQW equation. The ignition time, τ was determined by Eq.(1) with $\dot{q}''_e = \dot{q}''_f$, same as Eq. (32) used by Karlsson. $\dot{q}''_f$ was taken as 30 kWm^{-2} for the extended flame length in upward flame spread. The concurrent flame length, y_f (Eq. 46) was estimated by the linearized power-n correlation with K taken as 0.01 m^{2}kW^{-1}. The concurrent burnout position was determined by Eq. (47).

The lateral pyrolysis front (Eq. 48) was determined using the LIFT Eq. (15) for T_s higher than the minimum surface temperature for flame spread, $T_{s,\min}$ derived from the LIFT test. The lateral burnout front was determined similarly in concurrent flame spread (Eq. 49).

Downward spread only occurs at $t > t_H$ when $y_p = H$. The downward pyrolysis front (Eq. 50) and the downward burnout front (Eq. 51) at t'_H were obtained.

Once ignition occurs when $T_{s,o} = T_{ig}$, Eqs. (45) to (51) on the positions of flame fronts and burnout fronts are integrated by second-order Runga-Kutta method to give the total pyrolysis area, A_p (Eqs. 52 to 56). The total heat release rate can be obtained by Eq. (16).

6. FLAME SPREAD MODEL ON LIFT TEST

Both of the models developed by Karlsson and Quintiere require input data from the LIFT test. A model was developed by Qian [12] to model the transient surface temperature, flame front, burnout front and flame spread rate in LIFT by cone calorimeter data including the ignition time, critical surface temperature for ignition, heat release rate and flame duration. Assumptions were made for particular flame configuration, flame duration and emissivity.

The flame front was modelled by monitoring the surface temperature of the material, $T_s(x,t)$. $T_s(x,t)$ at every position along the material was calculated according to the imposed net heat flux which includes the external heat flux from the radiation panel, $\dot{q}''_e(x)$, the radiative heat flux from the flame after ignition, $\dot{q}''_f(x,t)$, and the natural convective heat loss to the ambient, $\dot{q}''_c(x,t)$. $T_s(x,t)$ was calculated by Duhamel integral. When $T_s(x,t) \geq T_{ig}$, there is ignition and the flame spread forward.

$$T_s(x,t) = T_o + 2\dot{q}''_e(x)\sqrt{\frac{t}{\pi k\rho c}} + \int_0^t 2\left\{\frac{\partial}{\partial t_p}\left[\dot{q}''_c(x,t_p)\right]\right\}\sqrt{\frac{t-t_p}{\pi k\rho c}}dt_p + 2\dot{q}''_f(x,t_{ph})\sqrt{\frac{t-t_{ph}}{\pi k\rho c}} + \int_{t_{ph}}^t 2\left\{\frac{\partial}{\partial t_p}\left[\dot{q}''_f(x,t_p)\right]\right\}\sqrt{\frac{t-t_p}{\pi k\rho c}}dt_p \quad (57)$$

t_{ph} is the preheating period specified in LIFT and there is no flame, i.e. $\dot{q}''_f = 0$ for $t < t_{ph}$. $\dot{q}''_c = -h(T_s - T_o)$ where h is the total heat loss coefficient. $\dot{q}''_f(x,t)$ is a function of the location of the flame end, $x_b(t)$ and the flame front, $x_f(t)$. The first value of x at which $T_s(x,t) < T_{ig}$ was defined as the location of the flame front, at $(t+\Delta t)$, i.e. $x_f(t+\Delta t)$. To determine the location of the "tail" of the flame, $x_b(t+\Delta t)$, the flame duration was calculated based on an empirical relation,

$$t_d = t_{d,cone} - \sum_i \sqrt{\frac{\dot{q}''_{cr} - \dot{q}''_{e,i}}{\dot{q}''_{cr}}}\sqrt{\frac{400 - \dot{q}''_{av}}{400}}\Delta t_i \quad (58)$$

t_d (in s) is the flame duration of the burning strip and $t_{d,cone}$ (in s) is the flame duration from cone calorimeter data. $\dot{q}''_{cr}$ (in kWm^{-2}) is the critical ignition irradiance for the material. $\dot{q}''_{av}$ (in kWm^{-2}) is the heat release rate of the material under 25 kW/m^2 from the cone calorimeter tests. 400 kWm^{-2} is the reference data taken as the PMMA data under 25 kW/m^2 from Cone tests. $\dot{q}''_{e,i}$ is the external irradiance at the position x. Δt_i is the difference of arrival time of the flame front between two adjacent burning strips, i.e. x and $(x+\Delta x)$. Eq. (58) is truly applicable for PMMA only and the effect of the variation of the equation for other materials should be studied in future.

In Qian's work, the radiation model treats the flame as a planar surface at a given flame height radiating to the unburned material with an emissivity, ε_f. The flame thickness, D was treated as the height of the emitting surface and the flame thickness correlation and shape factor are used to predict the radiative heat flux. Since the flame radiation is a volumetric effect, it is difficult to relate ε_f to the physical properties of the flame. This radiation model on the heat transfer from the flame to the unburned surface was improved [13] by Leung et al. by implementing a more realistic two-dimensional radiative transfer model and a simplified model of the luminous flame emissivity.

Several assumptions were made:

- The flame is a 2-D homogeneous gas/ particulates medium with temperature, T_f and particulates volume fraction, f_v.
- Gaseous radiation to the unburnt surface is small due to the small flame thickness.
- Luminous radiation emitted by soot particulates in the flame is the primary contribution to the radiative heating of the unburnt surface.
- Soot particulates are sufficiently small such that the Rayleigh's limit of particle absorption can be applied according to the Mie theory.

The gray soot model was used. The exchange factor between the flame and the differential area, dx at x was derived using a two-dimensional radiation function, $S_2(x)$, such that

$$F_{dx,g} = \int_0^1 \int_{\frac{x_b}{D}}^{\frac{x_f}{D}} \frac{aD\zeta S_2\left[aDs\left(\frac{x_f/D-\eta}{x/D-\eta}\right)\right]d\eta d\zeta}{s^2} \quad (59)$$

and $\dot{q}_f''$ was given by

$$\dot{q}_f'' = \alpha\sigma T_f{}^4 F_{dx,g}\left(aD, \frac{x_b}{D}, \frac{x_f}{D}, \frac{x}{D}\right) \quad (60)$$

where α is the absorptivity of the material surface, T_f is the flame temperature, a is the absorption coefficient, D is the flame thickness and aD is the optical thickness.

The model was used to simulate the flame spread in LIFT on expanded polystyrene, PMMA, birch faced plywood and fire retarded plywood. A sensitivity analysis was carried out on the effect of the optical thickness, aD on the prediction of the flame front, x_f. The results are shown in Fig. 4. It is apparent that the radiative emission from the flame has an important effect on the flame propagation behaviour. As the optical thickness of the flame increases, the flame spreads further and propagates with a higher rate. The improved radiation model was found to be useful for a good estimation of the contribution of the radiation feedback. The model was quite effective in simulating the flame spread rate. This can be further extended to model the flame spread process in other scenario such as ISO 9705.

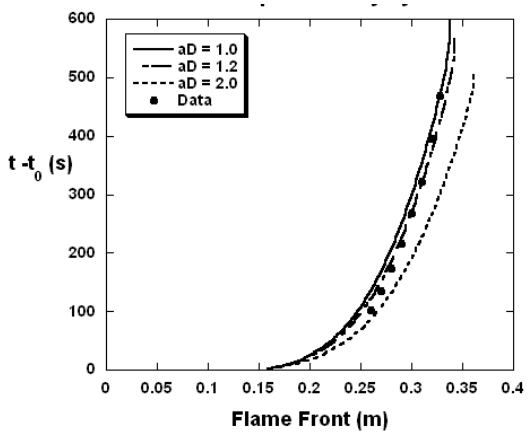

Fig. 4a: Comparison between the predicted flame front location with measurements for 40 mm expanded polystyrene [13]

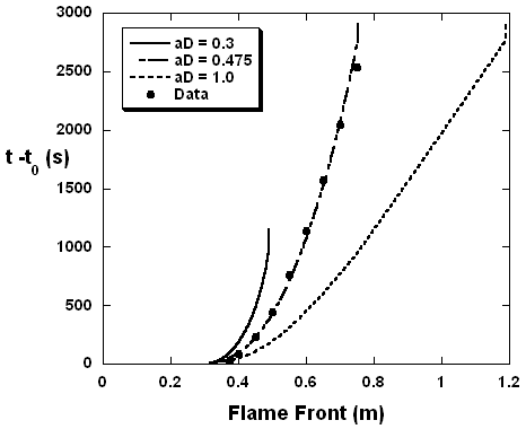

Fig. 4b: Comparison between the predicted flame front location with measurements for 3 mm PMMA [13]

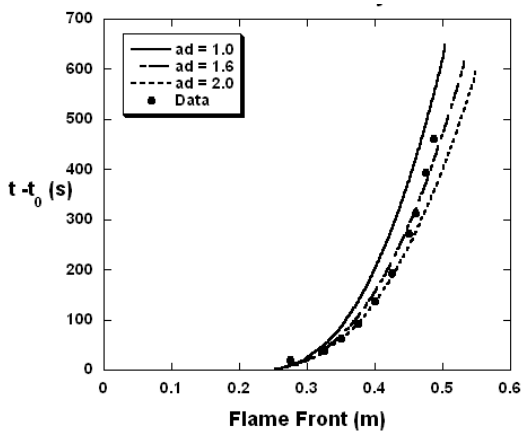

Fig. 4c: Comparison between the predicted flame front location with measurements for 9 mm birch face plywood [13]

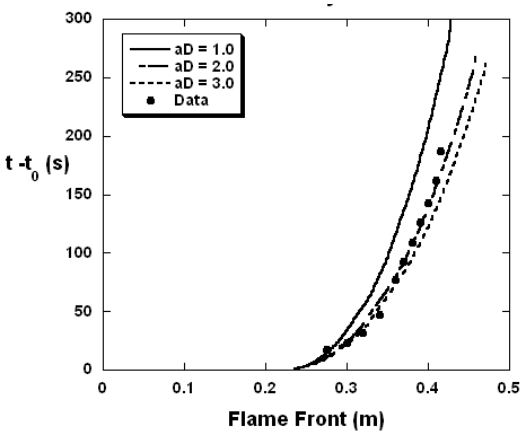

Fig. 4d: Comparison between the predicted flame front location with measurements for 4 mm FR plywood [13]

8. DISCUSSION

In concurrent flow flame spread problems, the ignition mechanism is dominated by the solid heating and gasification. Chemical kinetics effects are comparatively less important and are usually neglected in modelling. Simulation on those problems are based on analyzing the one-dimensional conduction heat transfer into the solid. The SQW equation developed by Saito, Quintiere and Williams [4] has been commonly used to model the rate of concurrent flow flame spread. Simulation on opposed flow flame spread problems require much knowledge on the gas phase chemical combustion reactions. Predictions on the lateral flame spread problems have been relied on the empirical equation obtained in the LIFT test [2,7]. The results are also applied on downward flame spread problems.

Göransson and Wichström [8] developed a simple model on heat release rate in ISO 9705 using empirical correlations on an effective surface temperature, gas temperature and burning area. This model is highly dependent on empirical constants and more experimental data should be obtained for further verifications.

Karlsson [9] used the SQW equation and the flame spread theories in LIFT to simulate the concurrent and downward flame spread in ISO 9705. Two scenarios were simulated, with one focusing on the concurrent flow flame spread along the vertical wall and beneath the ceiling and the other modelling the concurrent and opposed flow flame spread over the walls in the rooms. Quintiere also developed a model [10] on ISO 9705 using the SQW equation and LIFT theories. Both of the models assumed symmetric flame spread starting at the corner and constant heat flux from the flame and pyrolyzing material over the heated region beyond the pyrolysis front. Constant empirical figures independent of the properties of materials and the burning environment were used. The surface temperature, gas temperature, pyrolysis area and heat release rate in the room were simulated. The heat release rate was assumed to be consisted of the heat from the burner and the burning materials. The heat release rate from the materials was given by estimation on the pyrolysis area and approximations on heat release rate per unit area of the material determined in smaller scale tests like the cone calorimeter [11]. Mathematical approximation using the peak heat release rate of the materials with a decay function was used by Karlsson. This was criticized [5] as appropriate only for charring materials with slow decay in the local heat release rate. Quintiere used a correlation based on the total incident heat flux on the material and an effective material property derived from the heat of combustion and the effective heat of gasification. The pyrolysis area should be dependent on the flame front, pyrolysis front and burnout front. However, no burnout was considered in the original SQW equation and in Karlsson's model. It is not suitable for thin materials like linings and plastic materials with short burning time. Hasemi et al. [5] and Grant et al. [6] revised the SQW equation to include the burnout effects by adding a rectangular function of time and a characteristic burnout time respectively. The burnout effect was also considered in estimation of the pyrolysis area in Quintiere's model by defining the burnout front. Two different sets of boundary conditions and equations were used by Karlsson to obtain the surface temperature of materials inside and beneath the hot gas layer, while only an universal expression on surface temperature was used in Quintiere's model.

Qian [12] developed a model to simulate the flame spread rate in the LIFT test by using the data from the cone calorimeter. The flame was treated as a planar surface at a given flame height radiating to the unburned material. This was considered as not too adequate for reflecting the volumetric effect in the actual flame radiation. This was further modified by Leung et al. [13] using a two-dimensional radiative transfer model and a simplified model of the luminous flame emissivity. The new model was found to have better correlation with experimental results. Although radiation is less important in opposed flow flame spread, the concept used in the model and the improved radiation model can be extended to be used in modelling other scenarios like ISO 9705.

The solid heating, chemical kinetic mechanism and the conservation of mass, momentum, energy, species of pyrolyzing solid and reacting gases are complex problems difficult to analyse even individually. The flame spread models still rely much on input data from the cone calorimeter and LIFT test, experimental correlations on the flame length, gas temperature and opposed flow flame heating parameter; as well as simplifications like assumptions on constant heat flux from the flame and pyrolyzing materials, constant heat transfer and heat loss coefficients. Those assumptions might be over-simplified and this limits the application of the models on different materials, environmental conditions and testing scenarios.

Analytical models [e.g. 5,9] exert even more limitations on the input data and require more approximations. Fewer changes in the conditions are allowed such as the restriction on linearized flame length correlation, constant burner output at 100 kW in modelling ISO 9705. This can give very deviating results for those materials which only ignite at 300 kW burner heat exposure.

9. CONCLUSION

Flame spread is an important factor in controlling the fire hazard. It controls the rate of extension of the burning area and thus the heat release rate and even the time to flashover in a room.

In this paper, eight flame spread models were surveyed. Those include the concurrent flow models developed by Saito, Quintiere and Williams, Hasemi and Yasni, Grant and Drysdale, the opposed flow LIFT theories, the flame spread model for room-corner scenarios developed by Karlsson, Quintiere, Göransson and Wichström, the LIFT model developed by Qian and modified by Leung, Yuen and Chow. The key assumptions and equations in those models were summarized.

This paper introduced how to combine the theories on concurrent flow and opposed flow flame spread to model the flame spread processes in a full-scale room using bench-scale test data from LIFT and the cone calorimeter. Another model using cone calorimeter data to predict the flame spread rate in LIFT was also introduced. The techniques used in this model can be incorporated to model the flame spread problems in other scenarios.

There are still shortcomings and limitations in the existing models. Applications and correlations of the modelling results by Karlsson and Quintiere are still confined to the full scale ISO 9705 room corner fire. The models are not yet applied to other scenarios like rooms in different geometries and sizes. The potential applicability of the models is still unknown. Further improvements are needed and will be shown in future papers. More experimental works on full scale tests and even rooms in different configurations are also required for better correlations and verification of the models.

REFERENCES

1. A.C. Ferenandez-Pello, “Flame spread modelling”, Combustion Science and Technology, Vol. 39, pp. 119-134 (1984).
2. ASTM E1321-97a, Standard test method for determining material ignition and flame spread properties, American Society for Testing and Materials, West Conshohocken, USA (2002).
3. H.S. Carslaw and J.S. Jaeger, Conduction of heat in solids, Oxford University, Oxford (1959).
4. K. Saito, J.G. Quintiere and F.A. Williams, “Upward turbulent flame spread”, Proceedings of the First Symposium (International) on Fire Safety Engineering, Gaithersburg, MD, USA, pp. 75-96 (1985).
5. Y. Hasemi and N. Yasni, “A strategy to develop engineering upward flame-spread evaluation methodology based on the linearized flame height approximation”, Fire Science and Technology, Vol. 15, No. 1 & 2, pp. 17-28 (1995).
6. G. Grant and D. Drysdale, “Numerical modelling of early flame spread in warehouse fires”, Fire Safety Journal, Vol. 24, pp. 247-278 (1995).
7. J.G. Quintiere and M. Harkleroad, “New concepts for measuring flame spread properties”, NBSIR 84-2943, National Bureau of Standards, USA (1984).
8. U. Göransson and U. Wichström, “Flame spread predictions in the room/corner test based on the cone calorimeter”, Interflam ’90, Inter Science Communications Ltd, London, England, pp. 211-219 (1990).
9. B. Karlsson, “Modelling fire growth on combustible lining materials in enclosures”, Report TVBB-1009, Department of Fire Safety Engineering, Lund University, Lund, Sweden (1992).
10. J.G. Quintiere, “A simulation model for fire growth on materials subject to a room-corner test”, Fire Safety Journal, Vol. 20, pp. 313-339 (1993).
11. ISO 5660-1: 1993, Fire tests – Reaction to fire – Part 1: Rate of heat release from building products (cone calorimeter method), International Standards Organization, Geneva, Switzerland (1993).
12. J. Qian, “Prediction of flame spread test results from the test data of the cone calorimeter”, SP report 1990: 38, Swedish National Testing and Research Institute, Fire technology, Sweden (1990).
13. C.W. Leung, W.W. Yuen and W.K. Chow, “A practical model on flame spreading over materials”, The 6th ASME-JSME Thermal Engineering Joint Conference, 16-20 March (2003).
14. J.G. Quintiere, M. Harkleroad and Y. Hasemi, “Wall flames and implications for upward flame spread”, AIAA Paper No. 85-0456 (1985).
15. M.A. Delichatsios, “Flame height in turbulent wall fires with significant flame radiation”, Combustion Science Technology, Vol. 39, pp. 195-214 (1984).
16. K.M. Tu and J. G. Quintiere, “Wall flame heights with external radiation”, Fire Technology, Vol. 27, No. 3, pp. 195-203 (1991).
17. J.N. de Dis, “Spread of a laminar diffusion flame”, Proceedings of the Twelfth Symposium (International) on Combustion, The Combustion Institute, Pittsburgh, PA, USA, pp. 241-252 (1969).
18. ISO 9705: 1993(E), Fire tests – Full-scale room test for surface products, International Standards Organization, Geneva, Switzerland (1996).
19. C.W. Leung and W.K. Chow, “Recommendation on assessing flame spreading of materials using ISO 9705”, Fire Science and Technology, Vol. 23, No. 3, pp. 226-232 (2004).
20. B.J. McCaffrey, J.G. Quintiere and M.F. Harkleroad, “Estimating room temperature and the likelihood of flashover using fire test data

correlations", Fire Technology, Vol. 17, pp. 98-119 (1981).

21. B. Karlsson, "Room fires and combustible linings", SE-LUTVDG/TVBB-2050, Department of Fire Safety Engineering, Lund University, Lund, Sweden (1989).

22. P. Thomas and B. Karlsson, "On upward flame spread on thick fuels", Report LUTVDG/(TVBB 3058), Department of Fire Safety Engineering, Lund University, Lund, Sweden (1990).

23. W.J. Parker, "An assessment of correlations between laboratory and full-scale experiments for the FAA Aircraft fire safety program, Part 3; ASTM E84", NBSIR 82-2564, Center for Fire Research, Washington, DC, USA (1982).

24. ASTM E84-99, Standard test method for surface burning characteristics of building materials, American Society for Testing and Materials, West Conshohocken, USA (1999).

25. J.G. Quintiere, "A simulation model for fire growth on materials subject to a room-corner test", Presentation at the Fire Retardant Chemicals Association Spring Conference, Orlando, FL, USA (1992).

26. R.B. Williamson, A. Revenaugh and F.R. Mowrer, "Ignition sources in room fire tests and some implications for flame spread evaluation", Proceedings of the Third Symposium (International) on Fire Safety Engineering, Elsevier Applied Science, London, pp. 657-666 (1991).

27. B. Karlsson and S.E. Magnusson, "Combustible wall lining materials: Numerical simulation of room fire growth and the outline of a reliability based classification procedure", Proceedings of the Third Symposium (International) on Fire Safety Engineering, Elsevier Applied Science, London, pp. 667-678 (1991).